Applied Physics Research; Vol. 16, No. 1; 2024
ISSN 1916-9639 E-ISSN 1916-9647
Published by Canadian Center of Science and Education

Elastic Cross Section for the Reactions $^{235}U(n,n)$ and $^{238}U(n,n)$ at Low Energies Using Woods-Saxon and Coulomb Potentials

L. M. Sandoval[1], R. Arceo[1], G. León-Soto[2], O. Pedraza[3], J. Martínez-Castro[4] & L. A. López[3]

[1] Facultad de Ciencias en Física y Matemáticas, Universidad Autónoma de Chiapas, Chiapas, México
[2] Instituto de Investigaciones en Ciencias de la Tierra, Universidad Michoacana de San Nicolás de Hidalgo, Av. Francisco J. Múgica S/N, Edificio INICIT, Ciudad Universitaria, Michoacán, México
[3] Área Académica de Matemáticas y Física, Universidad Autónoma del Estado de Hidalgo, Mineral de la Reforma, México
[4] Centro de Investigación en Computación, Instituto Politécnico Nacional, Av. Juan de Dios Bátiz, esq. Miguel Othón de Mendizábal, Col. Nueva Industrial Vallejo, Delegación Gustavo A. Madero, Ciudad de México, México
Correspondence: R. Arceo, Facultad de Ciencias en Física y Matemáticas, Universidad Autónoma de Chiapas, C.P. 29050, Tuxtla Gutiérrez, Chiapas, México.

Received: October 26, 2023 Accepted: December 1, 2023 Online Published: February 7, 2024
doi:10.5539/apr.v16n1p34 URL: https://doi.org/10.5539/apr.v16n1p34

Abstract
The elastic cross section for neutrons by Uranium atoms is calculated for the reactions $^{235}U(n,n)$ and $^{238}U(n,n)$ in the regime of low energies using Coulomb and Woods-Saxon potentials. The parameters used in the calculations were chosen by comparison with experimental data previously published by reducing chi-square. Using the same parameters in the equations the ratio $^{238}U/^{235}U$ is calculated. The results are shown next to the experimental data to illustrate the agreement of the model in the range of energies from 1.5 keV to 1.0 MeV.

Keywords: scattering theory, total cross sections, potential models

1. Introduction

Since the neutron discovery by Chadwick in 1932 (Chadwick, 1932), neutrons have been used in scattering experiments for several decades (Carpenter & Lander, 2010). Given that neutrons lack electric charge, they weakly interact with matter (Ederth, 2018) and penetrate deeper into the nucleus of different isotopes. For energies of a few MeV, the reduced wavelength of a neutron-nucleus system is approximately of the same order of magnitude as the nucleus (Block et. al., 2010). Therefore, for these energies, neutrons are able to interact with atomic nucleus and neutron scattering is well suited for estimating cross sections at nuclear level.

In the present work, we have used the data from GMAP database (Carlson et. al., 2018) of the $^{238}U(n,n)$ and $^{235}U(n,n)$; then, we have found solutions to the Schroedinger equation with an optical Woods-Saxon potential in the low energy regime (Carlson et. al., 2018; Arceo et. al., 2020). A Woods-Saxon potential can be considered as a smoothed version of a barrier potential (Rojas & Villalba, 2005).

In order to find the best fitting parameters to the experimental data (Carlson et. al., 2018) from the Coulomb barrier, we use a model that reduced the chi-squared uncertainty for the choice of the parameters such as the depth of the potential well, the length surface thickness of the nucleus, and the nuclear radius. There are few theoretical models and experimental data carried out for the reactions $^{238}U(n,n)$ and $^{235}U(n,n)$ (Poenitz, 1981; Poenitz & Aumeier, 1997; Chadwick et. al., 2006, 2011; Brown et. al., 2018; Otuka et. al., 2014).

In section II, we present the theoretical framework of the dispersion S matrix and the Woods-Saxon potential used in the estimation of the total elastic cross section.

2. Theory

The radial Schroedinger equation was solved to calculate the scattering of neutrons by Uranium atoms using an optical Woods-Saxon potential. The calculations described in (Arceo et. al., 2020) are briefly summarized as it follows.

The Schroedinger equation is,

$$\left[-\frac{\hbar^2}{2\mu}\nabla^2 + V(r)\right]\Psi(\vec{r}) = E\Psi(\vec{r})\,, \tag{1}$$

where $\mu = \frac{m_1 m_2}{m_1+m_2}$ is the reduced mass for a system of two single particles, E is the energy and $V(r)$ is the radial effective potential.

We introduce $U(r)$ as,

$$\Psi(\vec{r}) = \Psi(r) = \frac{U(r)}{r}\,, \tag{2}$$

and using separation of variables in the Schroedinger equation (1), we obtain its radial component,

$$U_l^{''}(r) + \frac{2\mu}{\hbar^2}\left[E - V(r)\right]U_l(r) - \frac{l(l+1)}{r^2}U_l(r) = 0, \tag{3}$$

with

$$V(r) = V_C(r) + V_{WS}(r), \tag{4}$$

$$V(r) = -\frac{1.44Z_{1,2}}{r} + \frac{V_0 Z_{1,2}}{1+\exp(\frac{r-R}{a})}, \tag{5}$$

where r is the radius given in fm, $V(r)$ is the potential given in MeV and $Z_{1,2}$ is the atomic number of each nucleus. $V_C(r)$ is de Coulomb potential, and $V_{WS}(r)$ is the Woods-Saxon potential which will be described in the section 2.2.

The radial equation (equation (3)) takes the final form,

$$U_l^{''}(r) + \frac{2\mu}{\hbar^2}\left[E + \frac{1.44Z_{1,2}}{r} - \frac{V_0 Z_{1,2}}{1+\exp(\frac{r-R}{a})}\right]U_l(r) - \frac{l(l+1)}{r^2}U_l(r) = 0. \tag{6}$$

2.1 The Scattering S Matrix

The S matrix takes several mathematical forms (Gibbs, 2006). We used the form in which the solutions from the radial Schroedinger equation U_l (equation (6)) are introduced to include the scattering process for the reactions $^{238}U(n,n)$ and $^{235}U(n,n)$.

The numerical techniques used to solve the Schroedinger equation with a radial potential are explained in chapter 3, Equation (3.28) of (Gibbs, 2006) and in a section from (Arceo et. al., 2015, 2020, 2021), is summarized this procedure. The solutions of U_l from equation (6) are introduced in the S matrix (Eq. 10.58 of (Gibbs, 2006)), which is,

$$S_l = \frac{U_l(r_{n-1})r_n h_l^-(kr_n) - U_l(r_n)r_{n-1}h_l^-(kr_{n-1})}{U_l(r_n)r_{n-1}h_l^+(kr_{n-1}) - U_l(r_{n-1})r_n h_l^+(kr_n)}\,, \tag{7}$$

where the S matrix is evaluated in the last two points on a mesh of size δ (r = 0, δ, 2δ, ..., $n\delta$). U_l are the solutions to the Schroedinger equation with the potential previously calculated and h_l are the spherical Hankel functions defined in Eq. 10.52 of (Gibbs, 2006).

The scattering amplitude for a partial wave decomposition in terms of the S matrix is,

$$f(\theta) = \frac{1}{2ik}\sum_{l=0}^{\infty}(2l+1)P_l(cos\theta)(S_l - 1)\,. \tag{8}$$

For states with well defined spin and isospin, the total cross section for neutrons via Uranium atoms scattering into a solid angle element dΩ is given by the scattering amplitude $f(\theta)$ of the reaction

$$\sigma_T = \frac{4\pi}{k}Im[f(0^o)], \tag{9}$$

where k is the center-of-mass momentum and $f(0^o)$ is the forward amplitude.
The results from the dispersion are shown in the next section.

2.2 The Woods-Saxon Potential

The Woods-Saxon potential (Woods & Saxon, 1954) is used and explained in section 2.1 of (Arceo et. al., 2020),

$$V'(r^*) = -\frac{V_0}{1+\exp(\frac{r^*-R}{a})}, a \ll R \tag{10}$$

where V_0 is the potential well depth, a is the length surface, R is the nuclear radius, and r^* is the distance from the center of the nucleus.

In the Figure 1 the Woods-Saxon and the Coulomb potential are plotted as a function of r^*. We have used the parameters obtained in Table 1 and the equation (5).

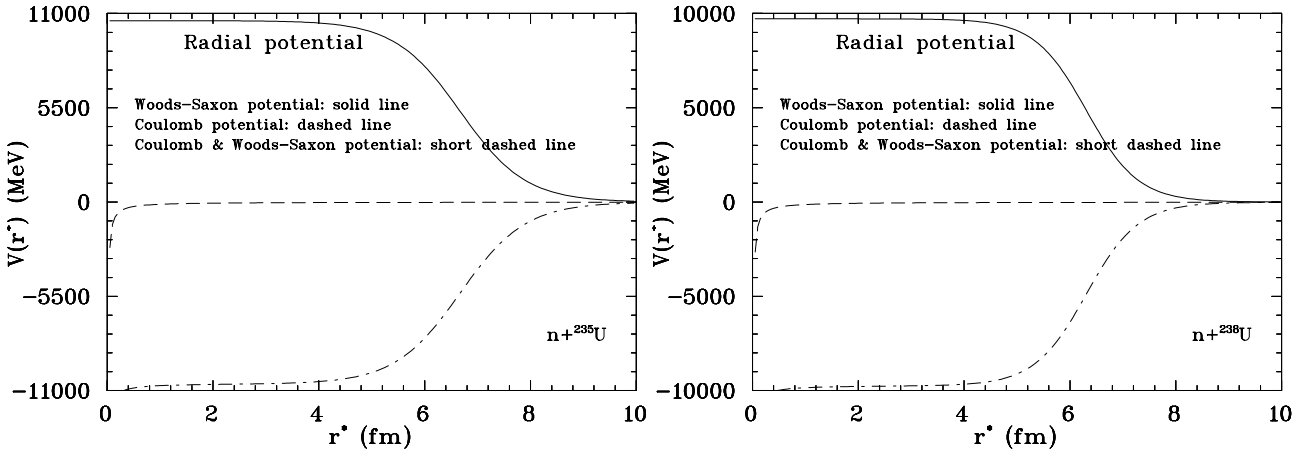

Figure 1. The solid line is for the Woods-Saxon potential, the dashed line is for the Coulomb potential, and the dashed-dot line is for the Woods-Saxon and Coulomb potential using the parameters from the Table 1

In Figure 2 is shown the results of the chi-squared calculations obtained with the variations of the parameters in the Woods-Saxon potential. In this case, we compare the experimental data from (Carlson et. al., 2018) with the proposed optical model. The parameters shown in Table 1 are in the range from 0 to 50 in the chi-squared distribution, this range corresponds to the larger count number.

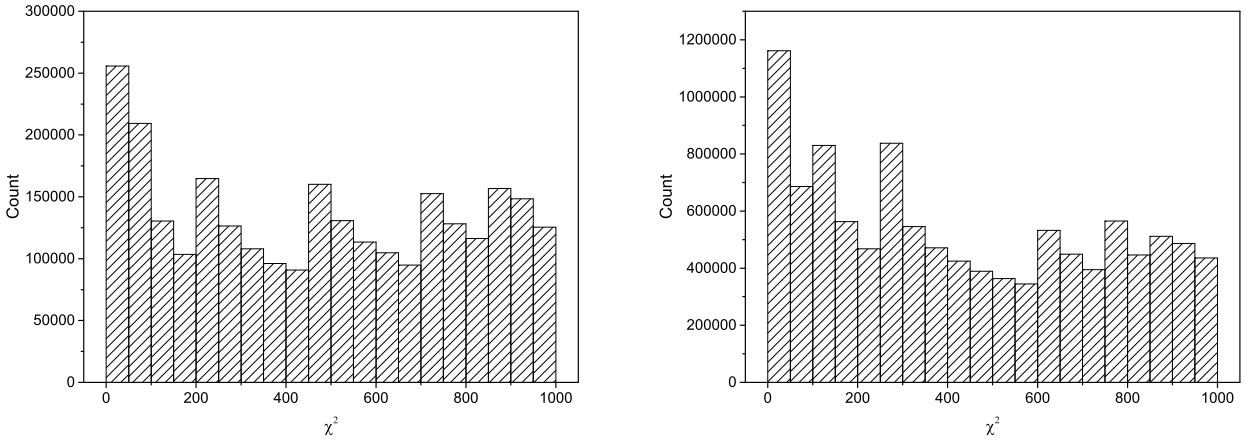

Figure 2. The χ^2 histogram for $^{235}U(n,n)$ (left plot) and the χ^2 histogram for $^{238}U(n,n)$ (right plot)

In the Table 1 are showed the parameters that minimize the chi-squared for the reactions $^{238}U(n,n)$ and $^{235}U(n,n)$ using the experimental data from (Carlson et. al., 2018).

Table 1. Parameters obtained for the reactions $^{238}U(n,n)$ and $^{235}U(n,n)$

Reaction	E (MeV)	l *up to*	V_0 (MeV)	R (fm)	a (fm)
$^{238}U(n,n)$	0-2.2	9	-105.60	6.31	0.489
$^{235}U(n,n)$	0-2.2	9	-115.00	6.67	0.616

3. Elastic Cross Section

The analysis is performed for the reactions $^{238}U(n,n)$ and $^{235}U(n,n)$ in the energy range from 1.5 keV to 1.0 MeV. We observe that the cross section decreases as the incident neutron energy increases.

Figure 3 shows the total cross section for the interaction of neutrons by Uranium isotopes. We evaluated the cross sections at energies up to E= 1.0 MeV by considering the radial effective Woods-Saxon and Coulomb potentials, and setting the parameters calculated by reducing the chi-squared in fitting the experimental data in (Carlson et. al., 2018) and shown in Table 1.

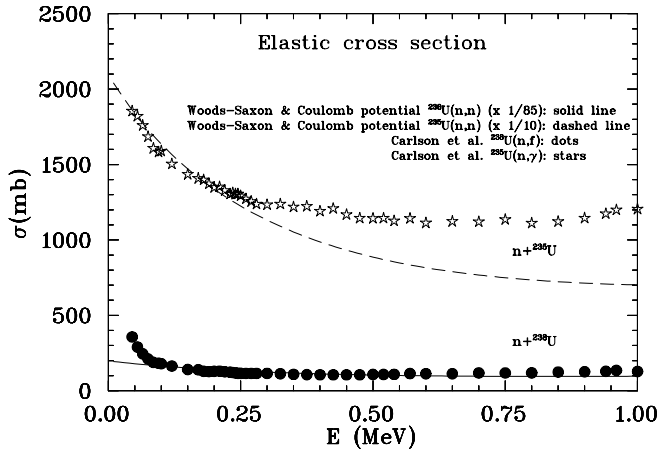

Figure 3. The elastic scattering cross sections for $^{238}U(n,n)$ and $^{235}U(n,n)$ are plotted as a function of the incident neutron energy. The experimental data were taken from (Carlson et. al., 2018)

In Figure 4 the total cross section ratio from $^{238}U(n,n)$ to 10 times $^{235}U(n,n)$ is plotted as a function of the incident neutron energy. The experimental data were taken from (Carlson et. al., 2018).

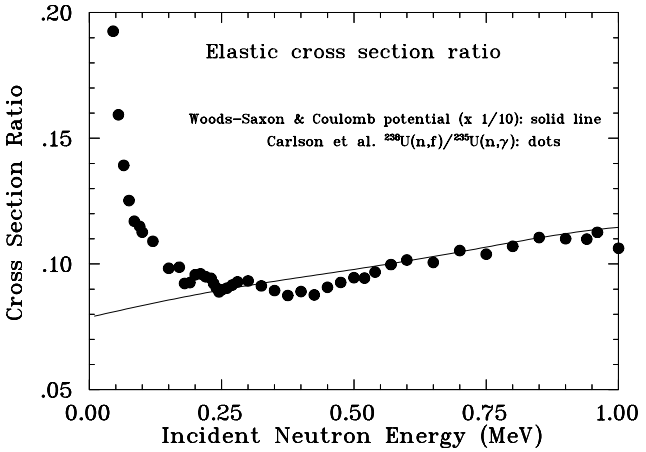

Figure 4. The elastic cross section ratio from $^{238}U(n,n)$ to 10 times $^{235}U(n,n)$ is plotted as a function of the incident neutron energy. The experimental data were taken from (Carlson et. al., 2018)

4. Conclusions

In this work, we have explored the radial Schroedinger equation with a central potential to analyze the dispersion of neutrons by Uranium isotopes at low energy regime. For this purpose, we used the central potential obtained by the addition of Coulomb and Woods-Saxon potentials. In the case of the Woods-Saxon potential, their parameters were obtained by minimizing the chi-squared (see Table 1). In Figures 3 and 4, we show a comparison between the numerical results and the corresponding experimental data in the interaction between the chosen Uranium isotopes and neutrons for the energy range between 1.5 keV and 1.0 MeV and their ratio. It is worth mentioning that our numerical analysis was made using a mesh of size δ = 0.05 fm.

In Figure 4, the total elastic cross section ratio $^{238}U/^{235}U$ is analyzed in a range from 0 to 1 MeV. The cross section ratio is useful since the $^{238}U(n,n)$ cross section is taken as a basis in the neutron flux measurements and can be used to improve the $^{235}U(n,n)$ cross section. Finally, the factors to fit the experimental data to our numerical fits are 1/85 for ^{238}U and 1/10 for ^{235}U for the elastic cross sections; and, 1/10 for the cross section ratio.

Acknowledgements

This work was partially supported by FCFM-UNACH. L. M. Sandoval acknowledges the postdoctoral fellowship received from CONACyT.

References

Arceo, R., Pedraza, O., González-Espinosa, E., Escalera Santos, G. J., & Díaz-Hernández, O. (2015). Elastic cross sections in an RSII scenario. *J. Phys. G: Nucl. Part. Phys., 42*, 015107 (9pp). Retrieved from https://iopscience.iop.org-/article/10.1088/0954-3899/42/1/015107

Arceo, R., Pedraza, O., Sandoval, L. M., López, L. A., Álvarez, C., Hueyotl-Zahuantitla, F., ... Martínez-Castro, J. (2020). Elastic Cross Sectios for ^3He+^{58}Ni above the Coulomb Barrier. *World Journal of Nuclear Science and Technology, 10(1)*, 1-8. https://doi.org/10.4236/wjnst.2020.101001

Arceo, R., Sandoval, L. M., Pedraza, O., López, L. A., León-Soto, G., & Martínez-Castro, J. (2021). Elastic scattering for π+p using the Klein–Gordon equation. *International Journal of Modern Physics E, 30*(6), 2150048 (13pp). https://doi.org/10.1142/S0218301321500488

Block, R. C., Danon, Y., Gunsing, F., & Haight, R. C. (2010). Neutron Cross Section Measurements. In Dan Gabriel Cacuci (Ed.), *Handbook of Nuclear Engineering*. Springer, Boston, MA. https://doi.org/10.1007/978-0-387-98149-9_1

Brown, D. A., Chadwick, M. B., Capote, R., ... Zhu, Y. (2018). ENDF/B-VIII.0: The 8th Major Release of the Nuclear Reaction Data Library with CIELO-project Cross Sections, New Standards and Thermal Scattering Data. *Nucl. Data Sheets, 148*, 1-142. https://doi.org/10.1016/j.nds.2018.02.001

Carlson, A. D., Pronyaev, V. G., Capote, R., Hale, G. M., ... Wang, W. (2018). Evaluation of the Neutron Data Standards. *Nuclear Data Sheets, 148*, 143-188. https://doi.org/10.1016/j.nds.2018.02.002

Carpenter, J. M., & Lander, G. H. (2010). 40 years of neutron scattering: a perspective. *Neutron News, 21*(1), 10-12. https://doi.org/10.1080/10448630903409152

Chadwick, J. (1932). Possible existence of a neutron. *Nature, 129*, 312. https://doi.org/10.1038/129312a0

Chadwick, M. B., Oblozinsky, P., Herman, M., Greene, N. M., ..., & van der Marck, S. C. (2006). ENDF/B-VII.0: Next Generation Nuclear Data Library for Nuclear Science and Technology. *Nucl. Data Sheets, 107(12)*, 2931-3060. https://doi.org/10.1016/j.nds.2006.11.001

Chadwick, M. B., Herman, M., Oblozinsky, P., Dunn, M. E., ... Young, P. G. (2011). ENDF/B-VII.1 Nuclear Data for Science and Technology: Cross Sections, Covariances, Fission Product Yields and Decay Data. *Nucl. Data Sheets, 112*(12), 2887-2996. https://doi.org/10.1016/j.nds.2011.11.002

Ederth, T. (2018). Neutrons for scattering: What are they, where to get them, and how to deal with them. *EPJ Web of Conferences, 188*, 01002 (23pp). https://doi.org/10.1051/epjconf/201818801002

Gibbs, W. R. (2006). *Computation in Modern Physics* (3rd ed.). World Scientific Publishing, Singapore.

Otuka, N., Dupont, E., Semkova, V., ... Zhuang, Y. (2014). Towards a More Complete and Accurate Experimental Nuclear Reaction Data Library (EXFOR): International Collaboration Between Nuclear Reaction Data Centres (NRDC). *Nucl. Data Sheets, 120*, 272-276. https://doi.org/10.1016/j.nds.2014.07.065

Poenitz, W. P. (1981). Data interpretation, objective evaluation procedures and mathematical techniques for the evaluation of energy-dependent ratio shape and cross section data. *Report BNL-NCS-51363, 1*, 249. Retrieved from https://digital.library.unt.edu/ark:/67531/metadc1113723/m1/1/

Poenitz, W. P., & Aumeier, S. E. (1997). The simultaneous evaluation of the standards and other cross sections of importance for technology. *Report ANL/NDM-139 (ANL, Argonne)*. United States: N. https://doi.org/10.2172/658382

Rojas, C., & Villalba, V. M. (2005). Scattering of a Klein-Gordon particle by a Woods-Saxon potential. *Phys. Rev. A, 71*, 052101 (4pp). https://doi.org/10.1103/PhysRevA.71.052101

Woods, R. D., & Saxon, D. S. (1954). Diffuse surface optical model for nucleon-nuclei scattering. *Phys. Rev., 95*, 577-578. https://doi.org/10.1103/PhysRev.95.577